1

RENGTH AND DUCTILITY OF CONFINED CONCRETE

By Murat Saatcioglu,[1] Member, ASCE, and Salim R. Razvi[2]

ABSTRACT: An analytical model is proposed to construct a stress-strain relationship for confined concrete. The model consists of a parabolic ascending branch, followed by a linear descending segment. It is based on calculation of lateral confinement pressure generated by circular and rectilinear reinforcement, and the resulting improvements in strength and ductility of confined concrete. A large volume of test data, including poorly confined and well-confined concrete was evaluated to establish the parameters of the analytical model. Confined concrete strength and corresponding strain are expressed in terms of equivalent uniform confinement pressure provided by the reinforcement cage. The equivalent uniform pressure is obtained from average lateral pressure computed from sectional and material properties. Confinement by a combination of different types of lateral reinforcement is evaluated through superposition of individual confinement effects. The descending branch is constructed by defining the strain corresponding to 85% of the peak stress. This strain level is expressed in terms of confinement parameters. A constant residual strength is assumed beyond the descending branch, at 20% strength level. The model is compared against a large number of column tests. Circular, square, and rectangular columns, with spiral and rectilinear reinforcements, as well as welded wire fabric, are used for comparison. Comparisons include concentric and eccentric loadings, as well as slow and fast strain rates. The results indicate good agreement.

INTRODUCTION

Confined concrete has stress-strain characteristics that are distinctly different than those of plain concrete. Prediction of stress-strain characteristics of confined concrete has been a topic for many researchers. Analytical models have been developed, usually on the basis of a specific set of test data. These models, although producing good predictions in many applications, have limitations in terms of cross-sectional shape and reinforcement arrangement (Sheikh 1982; Saatcioglu and Razvi 1991). Futhermore, the computational effort involved in some of the recent models is prohibitively excessive, sometimes implying undue accuracy. Therefore, there exists a need for a computationally attractive concrete confinement model that can be applied to the cross-sectional shapes and reinforcement arrangements used in practice.

An analytical procedure is presented in this paper based on equivalent uniform confinement pressure generated by the reinforcement cage. The pressure is quantified by using equilibrium of internal forces, and the results of experimental observations. The procedure recognizes potential differences in confinement pressures in two orthogonal directions, and allows for superposition of confinement effects of different types and arrangements of reinforcement. It is simple to use, and shown to produce good predictions of experimental data for circular, square, and rectangular sections confined with spirals, rectilinear hoops, cross ties, welded wire fabric, and combinations of different types of lateral reinforcement. The procedure is also shown to produce good predictions of concrete behavior [illegible] concentric and eccentric loadings, and slow and fast strain rates.

[1]Assoc. Prof., Dept. of Civ. Engrg., Univ. of Ottawa, Ottawa, Canada, K1N 6N5.
[2]Doctoral Student, Dept. of Civ. Engrg., Univ. of Ottawa, Ottawa, Canada.

Note. Discussion open until November 1, 1992. To extend the closing date one month, a written request must be filed with the ASCE Manager of Journals. The manuscript for this paper was submitted for review and possible publication on June 25, 1990. This paper is part of the ***Journal of Structural Engineering***, Vol. 118, No. 6, June, 1992. ©ASCE, ISSN 0733-9445/92/0006-1590/$1.00 + $.15 per page. Paper No. 26631.

CONFINED CONCRETE STRENGTH

Plain concrete subjected to longitudinal compression is in a uniaxial state of stress. Longitudinal strains generated by such loading give rise to transverse tensile strains that may result in vertical cracking. As the material approaches its uniaxial compressive capacity, the transverse strains and the vertical cracks reach their limiting values.

Combination of lateral pressure and axial compression results in a triaxial state of stress. Transverse strains caused by lateral pressure counteract the tendency of material to expand laterally, and result in increased strength. For a linearly elastic and isotropic material, the following relationship can be derived between uniaxial and triaxial stresses at a given lateral strain level:

$$\frac{-\mu f_{u2}}{E} = \frac{f_{t1} - \mu(f_{t2} + f_{t1})}{E} \quad (1)$$

$$f_{t2} = f_{u2} + k_1' f_{t1} \quad (2)$$

where

$$k_1' = \frac{1-\mu}{\mu} \quad (3)$$

where k_1' = a function of the Poisson's ratio μ, and results in higher values for lower values of this ratio; f_{t1}, f_{t2}, and f_{u2} = stresses under triaxial and uniaxial stress conditions, acting in directions 1 and 2; and E = the elastic modulus.

In reinforced concrete, the elastic modulus and Poisson's ratio vary with loading due to material nonlinearity. Furthermore, the stress-strain characteristics and Poisson's ratio may be different in all three orthogonal directions. Therefore, the aforementioned expressions are not applicable to concrete. However, an expression of the same form as (2) can be written to express triaxial strength of concrete in terms of uniaxial strength and lateral confinement pressure.

$$f'_{cc} = f'_{co} + k_1 f_l \quad (4)$$

where f'_{cc} and f'_{co} = confined and unconfined strengths of concrete in a member, respectively. While the coefficients k_1 and k_1' are not identical, it is reasonable to expect that k_1, like k_1', is a function of the Poisson's ratio, and as in the previous case, assumes lower values for higher values of this ratio. Since higher values of Poisson's ratio occur near failure, when the lateral pressure is maximum, lower values of coefficient k_1 correspond to higher values of lateral pressure.

The variation of coefficient k_1 with lateral pressure f_l can best be obtained from experimental data. Fig. 1 contains experimental data obtained from specimens subjected to different levels of hydrostatic pressure (Richart et al. 1928). The results show that coefficient k_1 does assume low values for high values of lateral pressure, approaching a constant value in the high pressure range. However, the lateral pressure provided by reinforcement is generally in the low end of the pressure range shown in Fig. 1. The expression

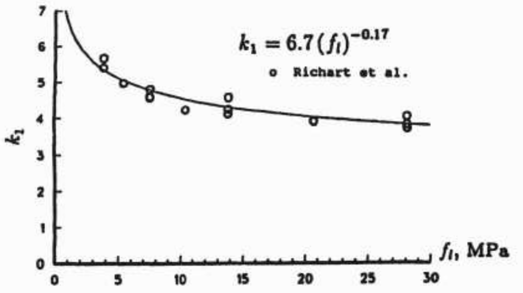

FIG. 1. Variation of Coefficient k_1 with Lateral Pressure

given herein, obtained from regression analysis of test data, reflects the variation of coefficient k_1 with lateral pressure.

$$k_1 = 6.7(f_l)^{-0.17} \quad (5)$$

where f_l = uniform confining pressure in MPa. The same trend was also observed by other researchers (Balmer 1949; Sato and Ibushi 1988).

Eq. (4) was also arrived at by Richart et al. (1928) from experimental data. Richart et al. (1928) performed a large number of cylinder tests under different levels of lateral fluid pressure, as well as tests of spirally reinforced cylinders (Richart et al. 1929). It was reported that (4) with a constant value of 4.1 for k_1 produced a good correlation with spirally reinforced test cylinders. Their recommendations have formed the basis of the confinement steel requirements of the ACI building code (*Building Code* 1989) for many years.

The unconfined concrete strength f'_{CO} in (4) is the plain concrete strength in a member under concentric loading. This may be different than that obtained from a standard cylinder test. Therefore it should best be determined from tests of plain concrete specimens of the same geometry, size, and concrete casting practice as those of the actual column member. In the absence of such test data, standard cylinder test results may be used with an appropriate modification. Modification factors ranging between 0.85 and 1.00 have been reported in the literature. For members subjected to high strain rates, the unconfined concrete strength f'_{CO} should be determined under the same strain rate for which the confined concrete strength f'_{CC} is sought.

Circular Sections

The relationship between concrete strength and lateral confining pressure given in (4) is valid for uniform lateral pressure. The pressure provided by closely spaced circular spirals and vertical column reinforcement can be considered to be uniform around the perimeter of the core. This lateral pressure can be computed from statics as illustrated in Fig. 2. If the pressure is computed at the useful limit of the hoop steel, i.e., at yield, and taken equal to the uniform pressure f_l given in (4), and coefficient k_1 is obtained from (5), confined concrete strength can be established for spirally reinforced circular columns.

Eq. (4) and (5) were used to predict confined concrete strengths of 15 circular columns reinforced with spiral and longitudinal reinforcements. The columns were tested under both slow and fast rates of concentric loading

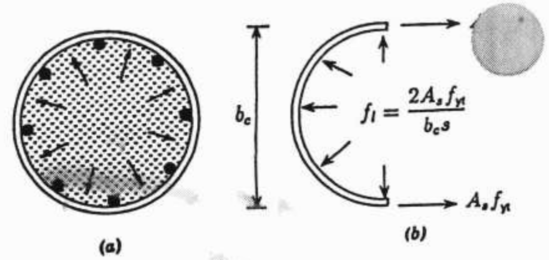

FIG. 2. Lateral Pressure in Circular Columns: (a) Uniform Buildup of Pressure; and (b) Computation of Lateral Pressure from Hoop Tension

TABLE 1. Strength Enhancement in Circular Columns

Column[a] label (1)	Reinforcement arrangement[b] (2)	f_l (MPa) (3)	k_1 (4)	k_2 (5)	f'_{CO} (MPa) (6)	$f'_{CC,exp}$ (MPa) (7)	$f'_{CC,anal}$ (MPa) (8)	$f'_{CC,anal}/f'_{CC,exp}$ (9)
a	10	3.08	5.53	1.00	24.0	38.0	41.0	1.08
b	10	3.38	5.45	1.00	30.0	48.0	48.4	1.01
c	10	3.38	5.45	1.00	32.0	47.0	50.4	1.07
1	10	4.28	5.23	1.00	29.0	51.0	51.4	1.01
2	10	2.54	5.72	1.00	29.0	46.0	43.5	0.95
3	10	1.70	6.12	1.00	29.0	40.0	39.4	0.99
4	10	0.96	6.75	1.00	29.0	36.0	35.5	0.99
5	10	3.17	5.51	1.00	29.0	47.0	46.5	0.99
6	10	3.06	5.54	1.00	29.0	46.0	45.9	1.00
7	10	3.38	5.45	1.00	32.0	52.0	50.4	0.97
8	10	3.38	5.45	1.00	30.0	49.0	48.4	0.99
9	10	3.38	5.45	1.00	32.0	52.0	50.4	0.97
10	10	3.38	5.45	1.00	30.0	50.0	48.4	0.97
11	10	3.38	5.45	1.00	30.0	54.0	48.4	0.90
12	10	3.38	5.45	1.00	32.0	52.0	50.4	0.97

[a]Tested by Mander et al. (1988). Column "a" was tested under slow strain rate, and all others under high strain rate of 0.0133/s.
[b]Reinforcement arrangements are illustrated in Fig. 5.

(Mander et al. 1988). The results are shown in Table 1. Comparisons of experimental and analytical values indicate excellent agreement.

Square Columns

While the uniform confining pressure for spirally reinforced columns can be found from the hoop tension, it is difficult to determine the confining pressure exerted by a square or a rectangular hoop. However, an approach analogous to that used for spirally reinforced columns can be employed based on equivalent lateral pressure, starting from material and geometric properties.

Passive confinement pressure exerted by a square hoop is dependent on the restraining force developed in the hoop steel. The hoop steel can develop high restraining forces at the corners, where it is supported laterally by transverse legs, and low restraining action between the laterally supported corners. The restraining force at the corners depends on the force that can be developed in the transverse legs, which, in turn, is related to the area and strength of the hoop steel. The restraining action of the hoop, between the corners is related to the flexural rigidity of the hoop steel, which depends on the size and unsupported length of the bar. This restraining action is

...rtional to the elastic rigidity of the hoop steel until yielding. Beyond ...g, the restraining action remains approximately constant until the strain hardening of steel produces additional restraining action. However, the flexural rigidity of the hoop between the laterally supported nodal points and the resulting restraining action is very small as compared to the restraining action of the corners and the other nodal points. Therefore, as the concrete expands laterally under axial compression, there will be higher reactive pressures building up at the nodal points than at locations away from the nodes. Fig. 3(*a*) illustrates the buildup of passive confinement pressure in a square column. If cross ties or inside hoops are used to support the middle bars, additional points of high lateral restraint are generated. It is clear that the shape of the pressure distribution is a function of the reinforcement arrangement. Shapes of pressure distributions for various tie arrangements are shown in Fig. 3(*b*).

Concrete confinement is a three-dimensional phenomenon that cannot be reduced to a sectional level. Therefore, it is essential to consider the variation of lateral pressure along the member length. This is illustrated in Fig. 4(*a*). It should be noted that the pressure developed at a nodal point, where the longitudinal bar is supported by a lateral tie is distributed reasonably uniformly along the length of the longitudinal bar. This is because the longitudinal bar in compression, with a short unsupported length between the ties, maintains the restraining action until shortly before it buckles. The lateral pressure between the ties reduces with the distance from the longitudinal reinforcement. This reduction occurs at a faster rate than that of the pressure at the tie level.

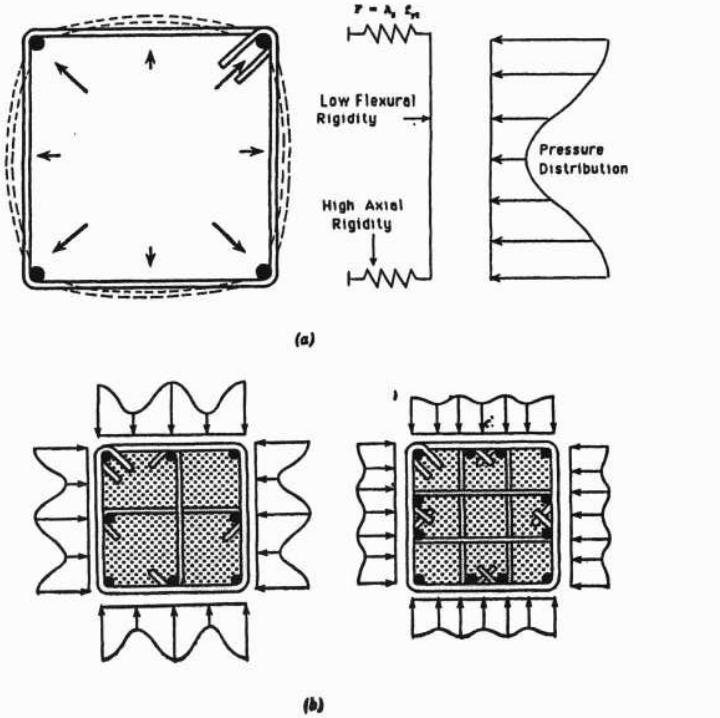

FIG. 3. Lateral Pressure in Square Columns: (*a*) Lateral Pressure Buildup in Square Columns; and (*b*) Pressure Distributions Resulting from Different Reinforcement Arrangements

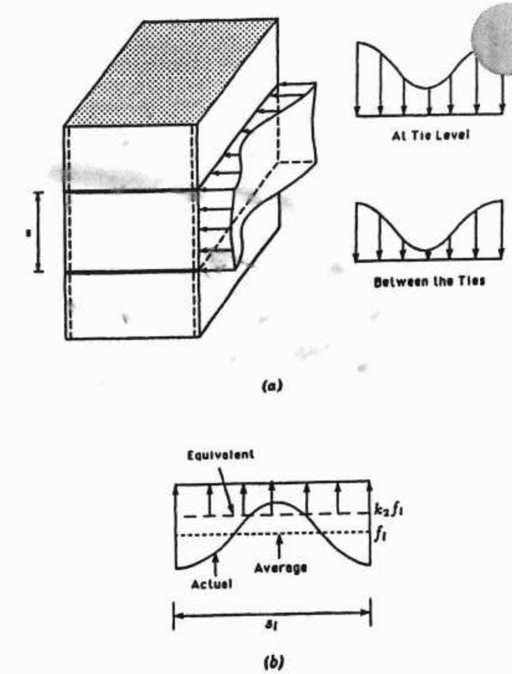

FIG. 4. Distributions of Lateral Pressures: (*a*) Distributions of Lateral Pressure along Member Length; and (*b*) Actual, Average, and Equivalent Lateral Pressures

For the case of closely spaced and laterally supported longitudinal reinforcement, the pressure distribution is close to uniform. In this case, a transverse force of $A_s f_{yt}$ is developed in each transverse bar at the useful limit of reinforcement, where A_s and f_{yt} are the area and yield strength of transverse reinforcement, respectively. The summation of these forces divided by the area bound by the core dimension, measured center to center of perimeter hoop (b_c) and center to center of tie spacing (s) leads to an average uniform pressure for which (4) was derived. At the other extreme, columns with four corner bars tied by perimeter hoops placed at large spacing are subjected to nodal forces at the corners. The reduction of pressure in the longitudinal direction between the ties becomes more pronounced. In this case, the assumption of uniform pressure, obtained by distributing these corner forces over the side of the core, results in overestimation of the actual effect of lateral pressure. Therefore, the average pressure cannot reflect the true effect of the actual confinement pressure. In this case an equivalent uniform pressure, with the same effect as that of the actual nonuniform pressure, is needed if (4) is to be used. Fig. 4(*b*) illustrates the actual, average, and equivalent lateral pressures in a square-column section. The equivalent uniform pressure f_{le} can be established by r[illegible]g the average pressure with due considerations given to the appro-p[illegible] parameters. Therefore, coefficient k_2 is introduced to reduce the average pressure. Eq. (4) then becomes

$$f'_{CC} = f'_{CO} + k_1 f_{le} \quad (6)$$

where

$$f_{le} = k_2 f_l \quad (7)$$

$$f_l = \frac{\Sigma A_s f_{yt} \sin \alpha}{s b_c} \quad (8)$$

$$k_1 = 6.7(f_{le})^{-0.17} \quad (9)$$

The equivalent lateral pressure in (9) is in MPa; $k_2 = 1.0$ for spirally reinforced circular columns as well as square columns with closely spaced lateral and laterally supported longitudinal reinforcement; and α = the angle between the transverse reinforcement and b_c, and is equal to 90° if the transverse reinforcement is perpendicular to b_c.

A large volume of experimental data was examined to define k_2. It is clear from the aforementioned discussion that k_2 should have a smaller value for large spacings of laterally supported longitudinal reinforcement (s_l) and ties (s) so that the reduction in the average stress is high. It was also found from experimental observations that a higher nodal force, resulting from large area and/or strength of transverse steel, increases stress concentration and sharpness of the stress peaks at the nodes. This requires further reduction in the average stress so that the stress regions away from the nodal points are not overestimated due to the sharpness of the stress peaks at the nodes. Therefore, coefficient k_2 is also a function of the average lateral pressure f_l. The following is the expression derived from regression analysis of test data:

$$k_2 = 0.26 \sqrt{\left(\frac{b_c}{s}\right)\left(\frac{b_c}{s_l}\right)\left(\frac{1}{f_l}\right)} \leq 1.0 \quad (10)$$

where f_l is in MPa. It should be noted that (10) is applicable only if premature buckling of longitudinal reinforcement is prevented. Based on the results of column tests considered in developing the aforementioned expression, the maximum tie spacing for buckling specified in the ACI building code (*Building Code* 1989) appears to satisfy this requirement. Furthermore, the columns considered conformed to the building-code limitation for maximum spacing of laterally supported longitudinal reinforcment. Therefore, this may be taken as an upper limit for s_l.

Eqs. (6)–(10) were used to predict confined concrete strengths of 49 square columns tested by three groups of researchers in three different research programs (Scott et al. 1982; Razvi and Saatcioglu 1989; Sheikh and Uzumeri 1980). The columns included a wide range of confinement parameters, ranging from poorly confined to well-confined columns. Different reinforcement configurations were used as indicated in Fig. 5. Both low and high rates of loadings were considered. Comparisons between the analytical and experimental strength values are presented in Table 2. The results indicate excellent agreement between the analytical and experimental values.

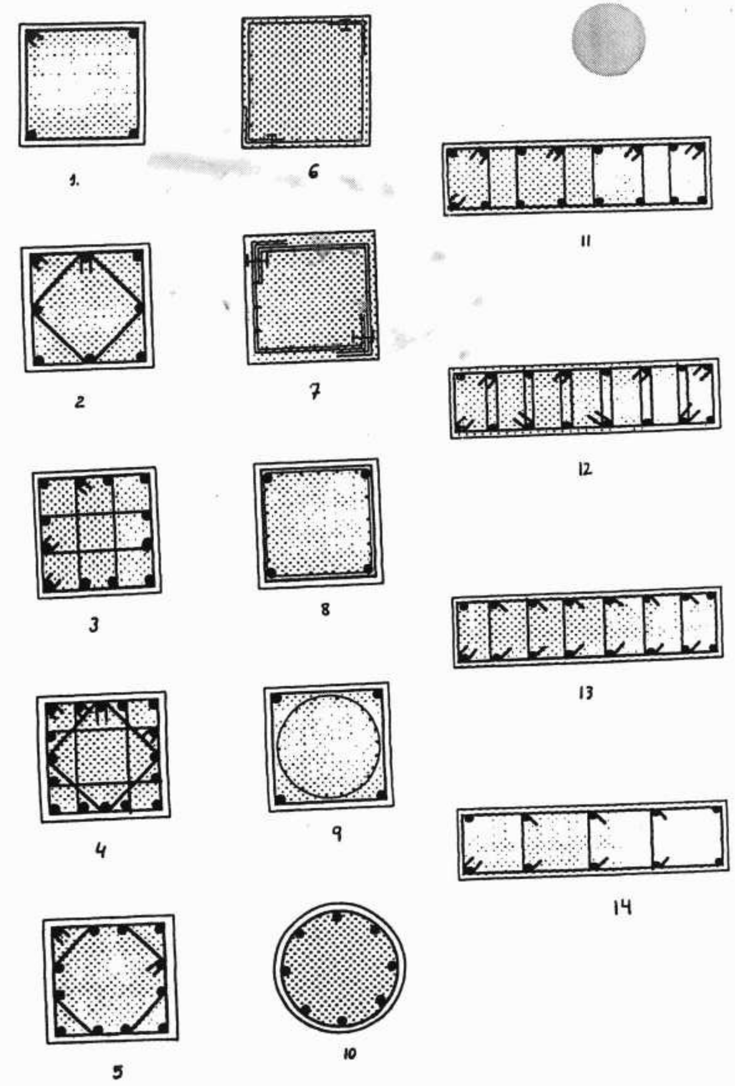

FIG. 5. Reinforcement Arrangements Considered in Tests

Rectangular Sections

Rectangular columns may have different confinement reinforcement in two orthogonal directions. This may lead to different levels of confinement pressure along the long and short sides of the section. The pressure along each side can be determined following the same procedure outlined previously for circular and square columns. Fig. 6 illustrates lateral pressure distributions along the long and short sides of a rectangular-column section. Confinement pressure along the long side plays a more dominant role on

TABLE 2. Strength Enhancement in Square Columns

Column[a] label (1)	Reinforcement arrangement[b] (2)	f_l (MPa) (3)	k_1 (4)	k_2 (5)	f'_{co} (MPa) (6)	$f'_{cc,exp}$ (MPa) (7)	$f'_{cc,anal}$ (MPa) (8)	$f'_{cc,anal}/f'_{cc,exp}$ (9)
3(a)	1	4.99	6.42	0.26	32.0	40.0	40.2	1.01
3(b)	1	4.99	6.42	0.26	32.0	38.4	40.2	1.05
4(a)	1	2.50	7.23	0.26	32.0	33.3	36.6	1.10
6(a)	1	5.17	6.44	0.24	39.0	51.9	47.1	0.91
6(b)	1	5.17	6.44	0.24	39.0	51.1	47.1	0.92
7(a)	1	2.59	7.25	0.24	39.0	43.3	43.6	1.01
7(b)	1	2.59	7.25	0.24	39.0	44.8	43.6	0.97
15(a)	1	2.50	7.23	0.26	29.0	35.1	33.6	0.96
15(b)	1	2.50	7.23	0.26	29.0	31.6	33.6	1.06
16(a)	1	4.99	6.42	0.26	29.0	38.0	37.2	0.98
16(b)	1	4.99	6.42	0.26	29.0	38.0	37.2	0.98
2	5	2.88	6.02	0.65	23.1	33.0	34.4	1.04
6	2	2.88	6.23	0.53	23.1	32.4	32.7	1.01
12	5	2.11	6.35	0.65	30.3	40.4	39.0	0.97
13	5	2.88	6.02	0.65	30.3	43.0	41.5	0.97
14	5	3.25	6.06	0.55	30.3	43.5	41.2	0.95
15	5	4.46	5.74	0.55	30.3	48.5	44.5	0.92
17	2	2.11	6.56	0.53	30.3	38.5	37.7	0.98
18	2	2.88	6.23	0.53	30.3	41.7	39.8	0.96
19	2	3.25	6.27	0.45	30.3	42.2	39.5	0.94
20	2	4.46	5.94	0.45	30.3	45.6	42.3	0.93
22	5	2.11	6.35	0.65	29.5	35.8	38.3	1.07
23	5	2.88	6.02	0.65	29.5	37.9	40.8	1.08
24	5	3.39	6.04	0.54	29.5	39.9	40.6	1.02
25	5	4.66	5.72	0.54	29.5	45.5	44.0	0.97
1	2	1.81	6.58	0.62	31.9	37.6	39.2	1.04
2	2	1.02	6.91	0.82	31.4	39.6	37.2	0.94
3	4	1.54	6.23	1.00	30.9	37.4	40.5	1.08
4	4	0.89	6.83	1.00	31.2	37.4	37.3	1.00
5	4	4.74	5.53	0.66	29.8	49.1	46.9	0.96
6	4	2.42	5.85	0.92	29.1	44.6	42.1	0.94
7	2	3.95	6.29	0.37	34.8	44.5	43.9	0.99
8	2	3.33	5.88	0.65	34.7	47.5	47.4	1.00
9	2	4.12	6.26	0.36	34.4	42.3	43.7	1.03
10	2	5.25	5.75	0.47	34.6	45.3	48.7	1.07
11	4	2.42	6.31	0.59	34.6	43.9	43.5	0.99
12	4	2.95	5.57	1.00	34.7	50.6	51.1	1.01
13	2	1.90	6.54	0.61	26.6	34.6	34.2	0.99
14	2	5.10	6.16	0.32	26.8	36.9	36.9	1.00
15	2	4.78	5.81	0.49	26.9	39.6	40.4	1.02
16	4	1.86	6.14	0.90	27.6	37.6	37.9	1.01
17	4	3.44	6.17	0.47	28.0	38.0	38.0	1.00
18	4	5.23	5.48	0.62	28.1	47.8	46.0	0.96
19	3	2.92	6.39	0.45	28.4	40.6	36.8	0.91
20	3	3.81	5.76	0.64	29.5	44.8	43.5	0.97
21	3	4.88	5.75	0.51	30.2	46.5	44.4	0.95
22	5	2.96	6.27	0.50	30.2	43.5	39.4	0.91
23	5	4.39	5.55	0.69	30.5	47.0	47.3	1.01
24	5	5.06	5.62	0.56	30.5	49.7	46.3	0.93

[a]From top to bottom: columns 3(a)–16(b) were tested by Razvi and Saatcioglu (1989); columns 2–25 were tested by Scott et al. (1982), where columns 12–25 were tested under high strain rate of 0.0167/s; and columns 1–24 were tested by Sheikh and Uzumeri (1980).
[b]For reinforcement arrangements see Fig. 5.

concrete strength than that along the short side. Examination of experimental data indicates that the effects of confinement pressures along the long and short sides can be considered to be proportional to the cross-sectional dimensions. Therefore, (11) can be used as overall equivalent lateral pressure to be used in (6).

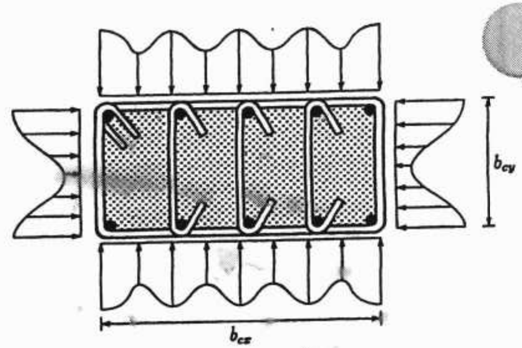

FIG. 6. Lateral Pressure Distribution in Rectangular Columns

TABLE 3. Strength Enhancement in Rectangular Columns

Column[a] label (1)	Reinforcement arrangement[b] (2)	$f_{l,long}$ (MPa) (3)	$f_{l,short}$ (MPa) (4)	$k_{2,long}$ (5)	$k_{2,short}$ (6)	k_1 (7)	f'_{co} (MPa) (8)	$f'_{cc,exp}$ (MPa) (9)	$f'_{cc,anal}$ (MPa) (10)	$f'_{cc,anal}/f'_{cc,exp}$ (11)
1	11	5.44	7.46	1.00	0.20	5.10	26	46	51	1.11
2	11	5.97	8.18	1.00	0.20	5.03	29	56	56	1.00
3	12	3.81	3.73	1.00	0.21	5.43	26	46	45	0.98
4	13	4.35	7.46	1.00	0.21	5.30	26	51	47	0.92
5	11	1.89	2.59	1.00	0.21	6.11	26	37	37	1.00
6	11	9.64	13.71	0.88	0.12	4.74	26	56	62	1.11
9	11	5.97	8.18	1.00	0.20	5.03	43	72	70	0.97
10	11	5.97	8.18	1.00	0.20	5.03	43	72	70	0.97
11	11	2.99	4.09	1.00	0.20	5.65	43	60	58	0.97
12	11	10.51	14.96	0.85	0.12	4.70	43	78	81	1.04
13	14	7.36	20.94	0.90	0.11	4.93	43	69	73	1.06
14	14	2.49	6.82	1.00	0.20	5.80	43	58	57	0.98

[a]Tested by Mander et al. (1988). Columns 1, 3, 5, and 6 were tested under slow strain rates, all others under high strain rate of 0.0133/s.
[b]Reinforcement arrangements are shown in Fig. 5.

$$f_{le} = \frac{f_{lex} b_{cx} + f_{ley} b_{cy}}{b_{cx} + b_{cy}} \qquad (11)$$

where f_{lex} and f_{ley} = effective lateral pressures acting perpendicular to core dimensions b_{cx} and b_{cy}, respectively. Eq. (11) also provides equivalent lateral pressure for square columns where the pressure distributions in two orthogonal directions are not equal.

Results of rectangular column tests conducted by Mander et al. (1988) are compared with analytical predictions of concrete strength obtained by the use of (6)–(11). The comparisons, shown in Table 3, indicate excellent agreement between the experimental and analytical strength values. The reinforcement arrangements used in the rectangular column tests are shown in Fig. 5.

Concrete Confined by WWF

The analytical procedure discussed can also be applied to columns reinforced with welded wire fabric. In this case, the column is treated the same as a column reinforced with reinforcing bars with due consideration given to the area and grid size of the welded wire fabric. The tie spacing is taken vertical grid dimension of the mesh. The spacing s_l between the ...ly supported longitudinal reinforcement is taken as the center-to-center distance between the outermost vertical wires unless there are lateral ties in between. Table 4 presents the comparisons of column test results (Abdulkadir and Saatcioglu 1991) and analytical predictions for columns reinforced with welded wire fabric.

Combined Use of Different Confinement Reinforcement

The analytical procedure presented also permits superposition of confinement effects resulting from the use of different types of confinement reinforcement. Razvi and Saatcioglu (1989) tested columns confined with welded wire fabric and square hoops (arrangements 8 and 9 in Fig. 5). The core concrete in these columns is confined by a combination of hoop and welded wire fabric reinforcement. The analytical procedure for this case involves computation of equivalent lateral pressures separately for each type of confinement reinforcement. The pressures acting over the same area are then superimposed to find the combined effect. This combined pressure is then used in (6) to find the confined concrete strength. In the cross-sectional arrangement 9 shown in Fig. 5, the inner circular core is subjected to uniform pressure provided by the welded wire fabric, and the equivalent uniform pressure provided by the outside hoops. In the same column, the core area between the outer hoops and the inside mesh is confined only by the outside hoops. Table 4 shows the comparison of analytical and experimental strength values.

The procedure employed in combining the effects of different types of confinement reinforcement is based on the superposition of equivalent uniform pressures, determined separately and independently. Therefore, the procedure does not take into account possible interaction effects between the confinement pressures and resultant changes in coefficient k_2.

Ductility of Confined Concrete

Plain concrete under uniaxial compression shows a brittle behavior. Deformability of concrete improves with confinement. Confined concrete can sustain higher strains at the peak load, and may show little strength decay thereafter.

The strain at peak stress is dependent on the effectiveness of confinement.

TABLE 4. Strength Enhancement in Columns Reinforced with Welded Wire Fabric

Column[a] label (1)	Reinforcement arrangement[b] (2)	$f_{l,WWF}$ (MPa) (3)	$f_{l,tie}$ (MPa) (4)	$k_{2,WWF}$ (5)	$k_{2,tie}$ (6)	k_1 (7)	f'_{co} (MPa) (8)	$f'_{cc,exp}$ (MPa) (9)	$f'_{cc,anal}$ (MPa) (10)	$f'_{cc,anal}/f'_{cc,exp}$ (11)
RC1	6	0.9	—	0.55	—	7.51	23	24	27	1.12
RC2	6	0.9	—	0.55	—	7.51	25	26	28	1.08
RC5	7	2.2	—	0.33	—	7.07	25	31	30	0.97
12(a)	9	0.9	2.5	1.00	0.26	6.24	29	40	37	0.93
12(b)	9	0.9	2.5	1.00	0.26	6.24	29	41	37	0.90
13(a)	9	0.8	2.5	1.00	0.26	6.28	29	38	37	0.97
13(b)	9	0.8	2.5	1.00	0.26	6.28	29	34	37	1.09
14(a)	8	0.6	2.4	1.00	0.27	6.50	29	38	37	0.97
14(b)	8	0.6	2.4	1.00	0.27	6.50	29	36	37	1.03

[a]Columns RC1–RC5 were tested by Abdulkadir and Saatcioglu (1991); and columns 12(a)–14(b) were tested by Razvi and Saatcioglu (1989).
[b]Reinforcement arrangements are shown in Fig. 5.

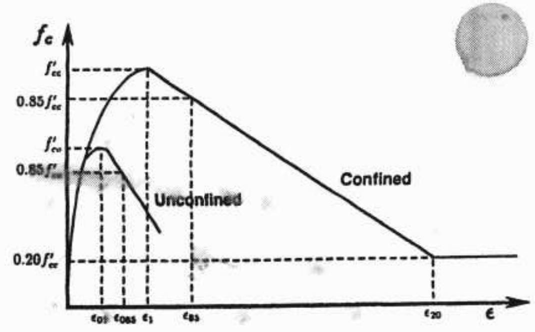

FIG. 7. Proposed Stress-Strain Relationship

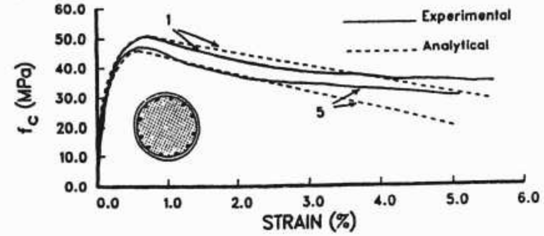

FIG. 8. Circular Columns Tested by Mander et al. (1988) under High Strain Rate of 0.0133/s

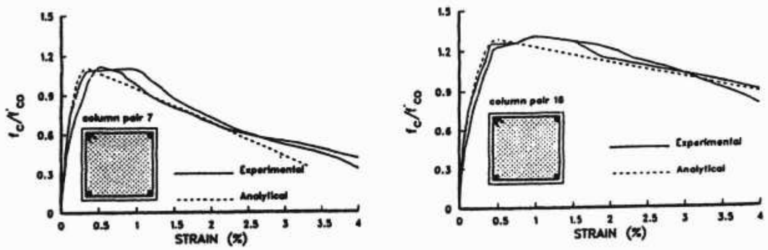

FIG. 9. Square Columns Tested by Razvi and Saatcioglu (1989) Under Slow Strain Rates

The following expression, also used by previous researchers (Balmer 1949; Mander et al. 1988) is found to produce good predictions of experimentally obtained strain values corresponding to peak stress (ε_1)

$$\varepsilon_1 = \varepsilon_{01}(1 + 5K) \quad (12)$$

where

$$K = \frac{k_1 f_{le}}{f'_{co}} \quad (13)$$

ε_{01} = the strain corresponding to peak stress of unconfined concrete, and

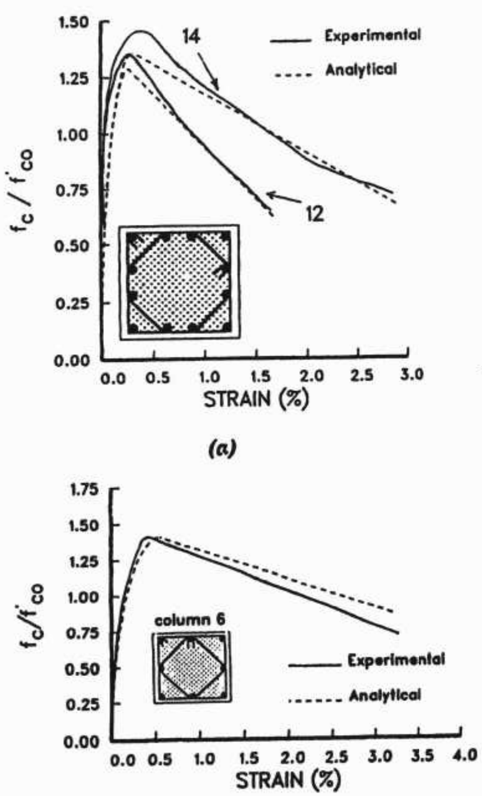

(a)

(b)

FIG. 10. **Square Columns Tested by Scott et al. (1982): (a) Tests under High Strain Rate of 0.0167/s; (b) Test under Slow Strain Rate**

should be determined under the same rate of loading as that used for the confined concrete. In the absence of experimental data, a value of 0.002 may be appropriate for ε_{01} under slow rate of loading.

Deformability of concrete beyond the peak stress is significantly affected by the behavior of longitudinal reinforcement. Longitudinal reinforcement in concrete is laterally restrained against buckling. However, spalling of cover concrete at approximately the peak stress level makes the longitudinal reinforcement susceptible to buckling. At this load stage, the lateral support provided by transverse reinforcement becomes important. If the amount of lateral reinforcement is sufficiently high in relation to the unsupported length of longitudinal reinforcement, the stability of longitudinal reinforcement between the ties is ensured. A stable reinforcement cage is essential to continue providing effective confinement against the lateral expansion of concrete. Therefore, the amount of transverse reinforcement, expressed in terms of reinforcement ratio (ρ), play a major role on the descending slope of the stress-strain relationship. Regression analysis of test data indicates

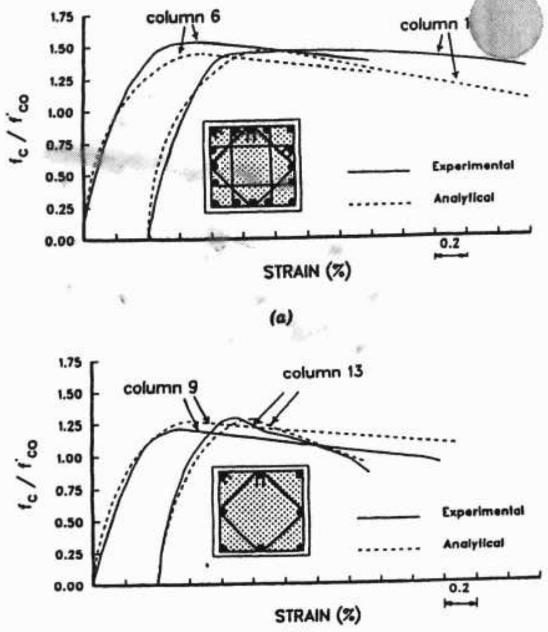

(a)

(b)

FIG. 11. **Square Columns Tested by Sheikh and Uzumeri (1980) under Slow Strain Rates**

that the following expression can be used to establish the strain at 85% strength level beyond the peak (ε_{85}).

$$\varepsilon_{85} = 260\rho\varepsilon_1 + \varepsilon_{085} \quad (14)$$

where

$$\rho = \frac{\Sigma A_s}{s(b_{cx} + b_{cy})} \quad (15)$$

ε_{085} = the strain at 85% strength level beyond the peak stress of unconfined concrete, and should be determined under the same rate of loading used for the confined concrete. In the absence of test data, a value of 0.0038 may be appropriate for ε_{085}, under slow rate of loading. The summation sign in (15) indicates the total area of transverse reinforcement in two directions, crossing b_{cx} and b_{cy}. If an inclined reinforcement is crossing the core, the projection of the area should be included in the total area. If the section is spirally reinforced, or has identical reinforcement arrangement in each direction, (15) reduces to that for transverse reinforcement ratio in one direction. In columns where more than one type of confinement reinforcement is used, the reinforcement ratio consists of the summation of reinforcement ratios for each type, computed with due consideration given to their respective core dimensions. It is important to note that, while the deformability of confined concrete improves with increasing transverse reinforcement ratio, it is not realistic to expect this improvement to continue

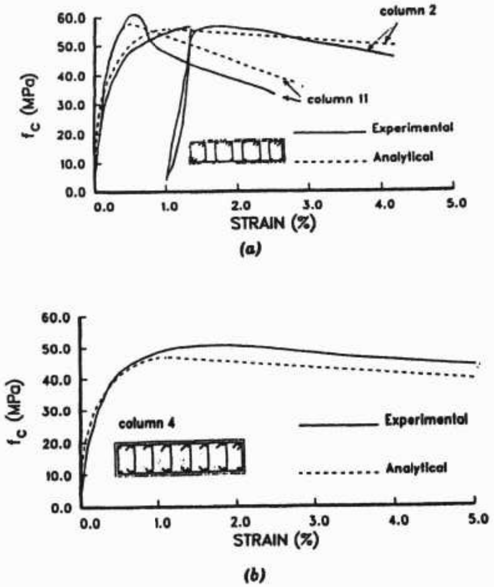

FIG. 12. Rectangular Columns Tested by Mander et al. (1988): (a) Tests under High Strain Rate of 0.0133/s; (b) Test under Slow Strain Rate

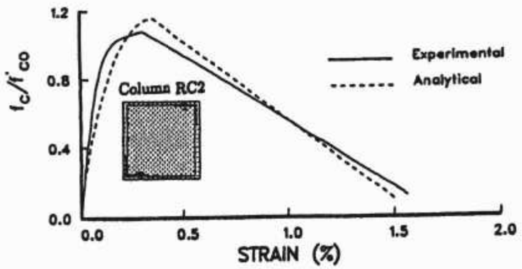

FIG. 13. Square Columns with Welded Wire Fabric, Tested by Abdulkadir and Saatcioglu (1991) under Slow Strain Rates

at the same rate, beyond the practical range of the reinforcement ratio. Eq. (14) was obtained from test data that included columns with less than 2% lateral reinforcement ratio. This may be used as an upper limit for (14).

Stress-Strain Relationship of Confined Concrete

The stress-strain relationship shown in Fig. 7 is proposed for confined concrete. The relationship consists of a parabola for the ascending branch, and a linear portion for the descending branch. A constant residual strength is assumed at 20% strength level. The following expression is suggested for the parabolic ascending portion.

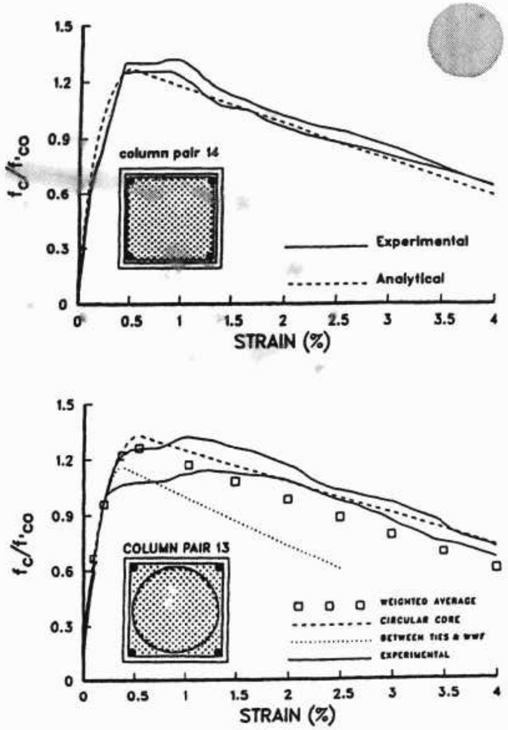

FIG. 14. Square Columns with Welded Wire Fabric and Hoops, Tested by Razvi and Saatcioglu (1989) under Slow Strain Rates

$$f_c = f'_{cc}\left[2\left(\frac{\varepsilon_c}{\varepsilon_1}\right) - \left(\frac{\varepsilon_c}{\varepsilon_1}\right)^2\right]^{1/(1+2K)} \leq f'_{cc} \quad (16)$$

where K is defined in (13). The proposed relationship becomes identical to that proposed by Hognestad (1951) for unconfined concrete, when confinement effects are negligible and the lateral confinement pressure is zero. This expression was selected for its simple and familiar form, even though under certain combinations of confinement parameters it may result in a slight underestimation of confined concrete stiffness prior to the onset of the concrete confinement mechanism.

The analytical relationship is compared with a large volume of experimental data, covering a wide range of confinement parameters between poorly confined and well-confined columns (Saatcioglu and Razvi 1991). Some of the typical comparisons are selected for presentation in Figs. 8–14 for circular, square, and rectangular columns tested under slow and fast rates of concentric compression. The comparisons indicate good correlation between the analytical and experimental results.

Additional comparisons are presented in Fig. 15 for columns tested under eccentric loading. Sectional analyses of two of the columns tested by Salamat and Saatcioglu (1991) under monotonically increasing eccentric loading were conducted using the proposed model. Moment-curvature relationships, ob-

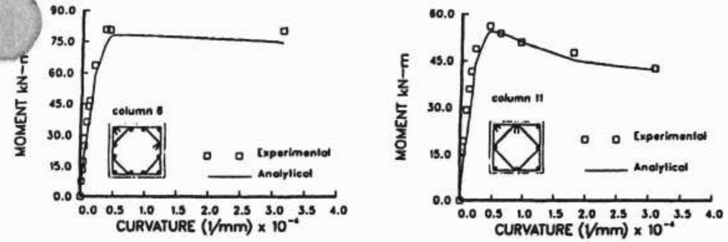

FIG. 15. Columns under Eccentric Loading, Tested by Salamat and Saatcioglu (1991) under Eccentric Loading

tained analytically, are compared with those obtained experimentally in Fig. 15. The comparisons indicate good predictions of column response under eccentric loading.

Conclusion

The analytical procedure presented in this paper provides a convenient means of establishing a stress-strain relationship for confined concrete. The procedure is relatively simple to use and general enough to cover the majority of concrete member shapes and confinement schemes used in practice. The stress-strain relationships established by the proposed procedure compare well with those obtained from column tests of different geometry and reinforcement, conducted under concentric and eccentric loading.

Appendix. References

Abdulkadir, R., and Saatcioglu, M. (1991). "Tests of concrete columns reinforced with welded wire fabric." *Research Report No. 9104*, Dept. of Civ. Engrg., Univ. of Ottawa, Ottawa, Canada.

Balmer, G. G. (1949). "Shearing strength of concrete under high triaxial stress-computation of Mohr's envelope as a curve." *Structural Research Lab. Report No. SP-23*, U.S. Bureau of Reclamation, Denver, Co.

Building code requirements for reinforced concrete and commentary. American Concrete Inst., Detroit, Mich., 353.

Hognestad, E. (1951). "A study of combined bending and axial load in reinforced concrete members." *Bulletin Series No. 399*, Univ. of Illinois Engrg. Experimental Station, Urbana, Ill.

Mander, J. B., and Priestley, M. J. N., Park, R. (1988). "Observed stress-strain behavior of confined concrete." *J. Struct. Engrg.*, ASCE, 114(8), 1827–1849.

Razvi, S. R., and Saatcioglu, M. (1989). "Confinement of reinforced concrete columns with welded wire fabric." *ACI Struct. J.*, 85(5), 615–623.

Richart, F. E., Brandtzaeg, A., and Brown, R. L. (1928). "A study of the failure of concrete under combined compressive stresses." *Bulletin No. 185*, Univ. of Illinois Engrg. Experimental Station, Urbana, Ill.

Richart, F. E., Brandtzaeg, A., and Brown, R. L. (1929). "The failure of plain and spirally reinforced concrete in compression." *Bulletin No. 190*, Univ. of Illinois Engrg. Experimental Station, Urbana, Ill.

Saatcioglu, M., and Razvi, S. R. (1991). "Analytical model for confined concrete." *Research Report No. 9101*, Dept. of Civ. Engrg., Univ. of Ottawa, Ottawa, Canada.

Salamat, A., and Saatcioglu, M. (1991). "Tests of confined columns under eccentric loading." *Research Report No. 9103*, Dept. of Civ. Engrg., Univ. of Ottawa, Ottawa, Canada.

Sato, T., and Ibushi, K. (1988). "Effect of confinement o[illegible]e behavior of reinforced concrete short columns." *Trans. of the Japan* [illegible]*te Inst.*, Japan Concrete Institute, 10(5), 337–344.

Scott, B. D., Park, R., and Priestley, M. J. N. (1982). "Stress-strain behavior of concrete confined by overlapping hoops at high and low strain rates." *ACI J.*, 79(1), 13–27.

Sheikh, S. A. (1982). "A comparative study of confinement models." *ACI J.*, 79(4), 296–305.

Sheikh, S. A., and Uzumeri, S. M. (1980). "Strength and ductility of tied concrete columns." *J. of Struct. Engrg.*, ASCE, 106(5), 1079–1102.